Electrochemistry in liquid sulfur dioxide. 12. Electrochemical and pulse radiolysis studies on oxidation of tris(2,2'-bipyridine)zinc(2+), tris(2,2'-bipyridine)cadmium(2+) and 2,2'-bipyridine

Jerzy B. Chlistunoff, and Allen J. Bard

Inorg. Chem., **1993**, 32 (16), 3521-3527 • DOI: 10.1021/ic00068a023

Electrochemistry in Liquid SO_2. 12. Electrochemical and Pulse Radiolysis Studies on Oxidation of $Zn(bpy)_3^{2+}$, $Cd(bpy)_3^{2+}$, and 2,2′-Bipyridine

Jerzy B. Chlistunoff† and Allen J. Bard*

Department of Chemistry and Biochemistry, The University of Texas at Austin, Austin, Texas 78712

Received November 13, 1992

The electrochemical oxidation of $Zn(bpy)_3^{2+}$, $Cd(bpy)_3^{2+}$, and 2,2′-bipyridine (bpy) in liquid sulfur dioxide was studied by cyclic voltammetry (CV) and spectroelectrochemical techniques. Both $Zn(bpy)_3^{2+}$ and $Cd(bpy)_3^{2+}$ are oxidized in three closely spaced one-electron reversible steps. The standard potentials for these processes referenced vs the ferrocenium/ferrocene couple are as follows: Zn, 2.33 ($E°_{3/2}$), 2.43 ($E°_{4/3}$), and 2.52 V ($E°_{5/4}$); Cd, 2.31 ($E°_{3/2}$), 2.39 ($E°_{4/3}$), and 2.47 V ($E°_{5/4}$). Additional multielectron irreversible oxidations were also seen for both complexes at potentials closer to the anodic background limit. The reversible processes were attributed to consecutive oxidations of the three bpy ligands to corresponding radical cations. The blue-colored $Zn(bpy)_2(bpy^{\bullet+})^{3+}$ was generated in a spectroelectrochemical cell and molar absorptivities (ϵ(391 nm) = 8790, ϵ(378 nm) = 4780, ϵ(762 nm) = 2570 M^{-1} cm^{-1}) were determined using the generation/decay data. As opposed to the $Zn(bpy)_2(bpy^{\bullet+})^{3+}$ spectrum, only one UV band centered around 340 nm was found in the transient spectrum of free $bpy^{\bullet+}$ (lifetime 1.2 μs) generated by electron pulse radiolysis of bpy in dichloromethane. The difference in properties is attributed to coordinated $bpy^{\bullet+}$ being a π-type radical while the free $bpy^{\bullet+}$ is probably a σ type radical. The $Zn(bpy)_2(bpy^{\bullet+})^{3+}$ ion dimerizes with a rate constant, k_2, of 70 M^{-1} s^{-1} at −70 °C. The $Cd(bpy)_2(bpy^{\bullet+})^{3+}$ ion was less stable.

Introduction

We consider here the oxidation of bipyridine (bpy) as a ligand compared to free bpy. The redox potential of a ligand and the stability of its oxidized (or reduced) form is often perturbed by complexation with a metal, just as the ligand modifies the behavior of the metal center. Stabilization of very low oxidation states of transition metals by bpy and related ligands has been the subject of many papers dealing with the properties of these complexes.[1] The effective oxidation state of a metal center in many of these strongly reduced species is higher than the formal oxidation state calculated from the electrical charge of the complex ion. Because of the extensive delocalization of the unpaired spin density over the ligands, these complexes are often considered as complexes containing ligand anion radicals in the coordination sphere.[1l] In most cases the electrostatic repulsion between negatively charged ligands is not strong enough to overcompensate attractive interactions, both specific and electrostatic, between the metal cation and the ligands. Consequently, coordinated anion radicals are weaker reductants than the free anion radicals. Moreover, a well-defined redox series, corresponding to consecutive one-electron reductions of the ligands, is observed.[1f-n] For example, the three reduction waves found with $Ru(bpy)_3^{2+}$ in acetonitrile can essentially be considered as reductions of the coordinated bpy ligands.[1i,j] Fewer studies have dealt with the oxidation of coordinated bpy ligands. In a series of previous reports, we have shown that electrogeneration of highly oxidized forms of metal bipyridine complexes containing bpy cation radicals in the coordination sphere is possible using liquid sulfur dioxide as a solvent.[2,3] This solvent offers the widest known anodic range for electrochemical studies and has been employed in a number of studies of highly oxidized species.[2-4] In contrast to radical anion complexes, the bonding between a radical cation and a metal cation is generally weaker than bonding between a metal cation and a neutral ligand. As a consequence, coordinated radical cations are stronger oxidants than the free radical cations. However, their reactivity in typical radical reactions, e.g., dimerization, is significantly reduced because of the relatively strong interactions with the metal cation. This increased stability of the radical, when it is coordinated to the metal cation, provides a unique opportunity to study unstable organic radicals by relatively simple nontransient experimental techniques. However, strong interactions between the radical and the metal ion can affect the individual properties of the radical especially when strong covalent bonding takes place. This is probably the case with known $bpy^{\bullet+}$ complexes with Fe(III), Ru(III), Os(IV), and Ni(IV).[2,3] In this paper, we report the results of electrochemical, spectral, and pulse radiolysis studies on the 2,2′-bipyridine cation radical and its complexes with Zn(II) and Cd(II) and discuss the effect of complexation on the properties of $bpy^{\bullet+}$ and possible mechanisms of its decomposition.

Experimental Section

Apparatus. Most of the electrochemical and spectroelectrochemical experiments were carried out with a PAR Model 173 potentiostat, a Model 175 universal programmer, and a Model 179 digital coulometer (Princeton Applied Research Corp., Princeton, NJ) employing positive feedback for *iR* compensation. The voltammograms for scan rates below 0.5 V s^{-1} were measured with a Model 2000 X-Y recorder (Houston

† On leave from the Department of Chemistry, University of Warsaw, Poland.

(1) (a) Kœnig, E.; Lindner, E. *Spectrochim. Acta* **1972**, *28A*, 1393. (b) Kœnig, E.; Herzog, S. *J. Inorg. Nucl. Chem.* **1970**, *32*, 585. (c) Kœnig, E.; Herzog, S. *J. Inorg. Nucl. Chem.* **1970**, *32*, 601. (d) Kœnig, E.; Herzog, S. *J. Inorg. Nucl. Chem.* **1970**, *32*, 613. (e) Hanazaki, I.; Nagakura S. *Bull. Chem. Soc. Jpn.* **1971**, *44*, 2312. (f) Saji, T.; Aoyagui, S. J. *J. Electroanal. Chem. Interfacial Electrochem.* **1975**, *58*, 401. (g) Tanaka, N. *Electrochim. Acta* **1976**, *21*, 701. (h) Hughes, M. C.; Rao, J. M.; Macero, D. J. *Inorg. Chim. Acta* **1979**, *35*, L231. (i) Tokel-Takvoryan, N. E.; Hemingway, R. E.; Bard, A. J. *J. Am. Chem. Soc.* **1973**, *95*, 6582. (j) Chen, Y. D.; Santhanam, K. S. V.; Bard, A. J. *J. Electrochem. Soc.* **1981**, *128*, 1460. (k) Richert, S. A.; Tsang, P. K. S.; Sawyer, D. T. *Inorg. Chem.* **1989**, *28*, 2471. (l) Creutz, C. *Comments Inorg. Chem.* **1982**, *1*, 293 and references therein. (m) Kahl, J. L.; Hanck, K. W.; DeArmond, K. *J. Phys. Chem.* **1978**, *82*, 540. (n) Kew, G.; DeArmond, K.; Hanck, K. W. *J. Phys. Chem.* **1974**, *78*, 727.

(2) (a) Gaudiello, J. G.; Sharp, P. R.; Bard, A. J. *J. Am. Chem. Soc.* **1982**, *104*, 6373. (b) Gaudiello, J. G.; Bradley, P. G.; Norton, K. A.; Woodruff, W. H.; Bard, A. J. *Inorg. Chem.* **1984**, *23*, 3. (c) Garcia, E.; Kwak, J.; Bard, A. J. *Inorg. Chem.* **1988**, *27*, 4377.

(3) Chlistunoff, J. B.; Bard, A. J. *Inorg. Chem.* **1992**, *31*, 4582.

(4) (a) Garcia, E.; Bard, A. J. *J. Electrochem. Soc.* **1990**, *137*, 2752. (b) Jehoulet, C.; Bard, A. J. *Angew. Chem., Int. Ed. Engl.* **1991**, *30*, 836. (c) Dietrich, M.; Mortensen, J.; Heinze, J. *Angew. Chem., Int. Ed. Engl.* **1985**, *24*, 508 and references therein. (d) Anson, F. C.; Collins, T. J.; Gipson, S. L.; Keech, J. T.; Krafft, T. E. *Inorg. Chem.* **1987**, *26*, 1157. (e) Ofer, D.; Crooks, R. M.; Wrighton, M. S. *J. Am. Chem. Soc.* **1990**, *112*, 7869 and references therein.

0020-1669/93/1332-3521$04.00/0

Instruments Inc., Houston, TX). Fast scan (scan rates, v, of 5–10 000 V s^{-1}) voltammograms were recorded using a homemade bipotentiostat, a PAR Model 175 universal programmer, and a Norland Model 3001/DMX storage oscilloscope. The low-temperature Dewar type spectrophotometrical cell of 8-mL volume described previously[3] was employed in spectroelectrochemical experiments. The solution in the cell was stirred with a magnetic stirrer.

The working electrode in low-scan-rate (0.03–0.5 V s^{-1}) voltammetric experiments was a 0.5-mm-diameter platinum disk electrode; at high scan rates (v > 0.5 V s^{-1}), 10- and 25-μm platinum microdisks were employed. The method of preparation of the microelectrodes has been described elsewhere.[2c]

A platinum gauze (3 cm × 5 cm) was used as a working electrode in coulometric and spectroelectrochemical experiments. The counterelectrodes were a piece of reticulated vitreous carbon (RVC) (1.5 cm × 1 cm × 1 cm) in coulometric studies and a piece of Pt gauze (2 cm × 2 cm) in spectroelectrochemical and voltammetric experiments. The counterelectrode for spectroelectrochemical studies was placed in 8-mm-diameter glass tubing and was separated from the working electrode compartment by a medium porosity glass frit.

The silver quasireference electrode (AgQRE) was always placed either in 1-cm-diameter glass tubing (coulometry and voltammetry) or in 3-mm-diameter shrinkable Teflon tubing (spectroelectrochemistry) and was separated from the solution of the working electrode compartment by a fine porosity glass frit.

The UV–vis spectra were measured on a Hewlett-Packard Model 8450A diode-array spectrophotometer. The pulse radiolysis experiments were performed at The University of Texas Center for Fast Kinetics Research and employed a Van de Graaf generator producing 4 MeV electrons at 10–20 Gy. All spectra are normalized for dose.

Chemicals. Tetra-*n*-butylammonium hexafluorophosphate, $(TBA)PF_6$, (Southwestern Analytical Chemicals Inc., Austin, TX) was purified by dissolution in acetone and precipitation with water six times, followed by recrystallization from an ethanol/ether mixture and then from an acetone/ether (1:5) mixture. Tetra-*n*-butylammonium hexafluoroarsenate, $(TBA)AsF_6$, was prepared and purified as described previously.[2c]

$Zn(bpy)_3(PF_6)_2$ and $Cd(bpy)_3(PF_6)_2$ were prepared by mixing an aqueous solution of 2,2′-bipyridine and $ZnCl_2$ (Aldrich, Milwaukee, WI) or $Cd(NO_3)_2$ (Fisher, Fair Lawn, NJ), respectively, (molar ratio 1:3.1) with a slight excess of KPF_6 (Sigma Chemical Co., St. Louis, MO) solution. The resulting precipitate was rinsed with distilled water, dried under vacuum, and recrystallized twice by slow evaporation of an acetonitrile/ethanol (1:1) solution.[5] The crystals were dried under vacuum at 60–70 °C for 72 h. 2,2′-Bipyridine (Aldrich, Milwaukee, WI) was purified by vacuum sublimation and stored in a drybox. Anhydrous SO_2 (Matheson Gas Products, Inc., Houston, TX) was purified as described previously.[2c]

Procedures. Procedures for the electrochemical experiments in liquid sulfur dioxide have been described elsewhere.[2c,3] Preparation for the spectroelectrochemical experiments consisted of drying the cell and electrodes at 160 °C followed by a 24-h evacuation of the cell with a predried sample of the supporting electrolyte (130 °C under vacuum) and the complex (70 °C under vacuum) on a vacuum line at ambient temperature.

The samples of bpy for electrochemical experiments were prepared in a drybox and sealed under vacuum in glass capillaries, which were placed in the cell and broken after condensing in sulfur dioxide. The $Zn(bpy)_3(PF_6)_2$, $Cd(bpy)_3(PF_6)_2$, and bpy solutions in methylene chloride for pulse radiolytic experiments were prepared by distilling CH_2Cl_2 (PHOTREX, J. T. Baker Inc., Phillipsburg, NJ) on a vacuum line from a CH_2Cl_2/CaH_2 mixture directly into glass ampules containing samples of the compounds. The ampules were opened before the experiments, and the solutions were transferred to the bubbling flasks equipped with Teflon valves and then purged with dry nitrogen saturated with CH_2Cl_2 for 20 min. The flasks were then connected under positive pressure of nitrogen to the 2-cm long flow through quartz cuvettes used in the experiments.

Results

Cyclic Voltammetry of $Zn(bpy)_3(PF_6)_2$, $Cd(bpy)_3(PF_6)_2$, and bpy. The electrode reactions of $Zn(bpy)_3^{2+}$ and $Cd(bpy)_3^{2+}$ were studied with SO_2 solutions 2–10 mM in $Zn(bpy)_3(PF_6)_2$ or $Cd(bpy)_3(PF_6)_2$, with either $(TBA)AsF_6$ or $(TBA)PF_6$ as supporting electrolytes. Two separate groups of waves appear on voltammograms of both complexes. One group of peaks appears at 2.3–2.5 V vs AgQRE and the second at potentials more positive than +3 V vs AgQRE (Figure 1). The first oxidation wave of $Zn(bpy)_3^{2+}$ is actually composed of three closely spaced anodic waves. Three corresponding cathodic waves were also seen on the voltammograms (Figure 2a). Within the scan rate range of 0.03–50 V s^{-1}, the first system of peaks behaved like a superposition of three one-electron reversible systems (Figure 2a). The anodic

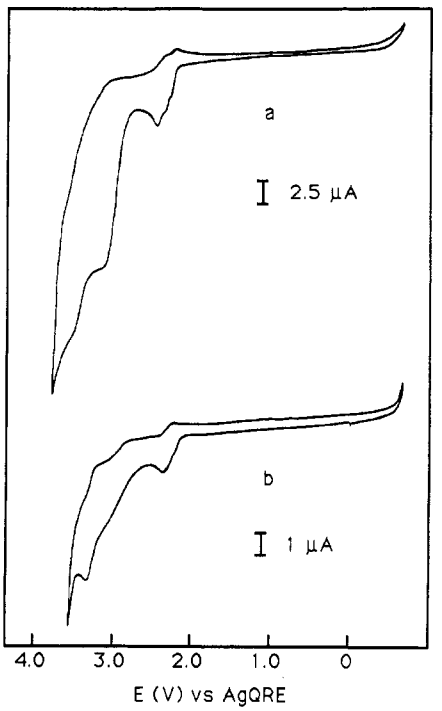

Figure 1. Typical voltammograms recorded for 8.8 mM $Zn(bpy)_3(PF_6)_2$ (a) and 2.2 mM $Cd(bpy)_3(PF_6)_2$ (b) in liquid sulfur dioxide at −70 °C. Background electrolyte: 0.1 M $(TBA)PF_6$. Scan rate: 0.2 V s^{-1}. Working electrode: 0.5-mm Pt disk.

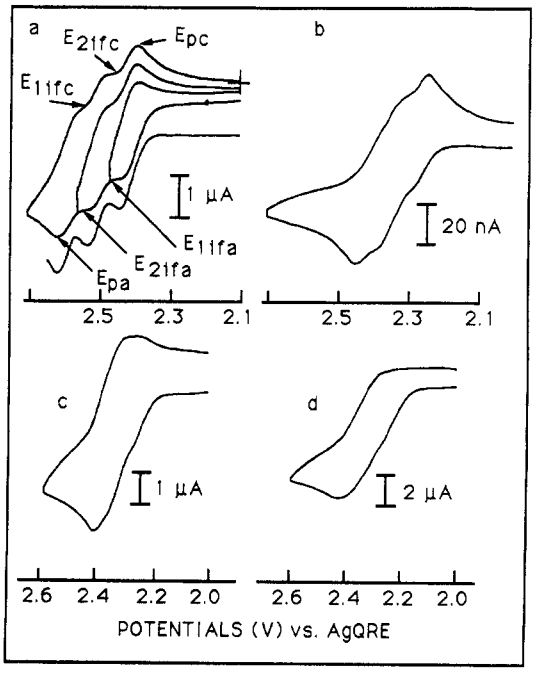

Figure 2. Voltammograms recorded for the first oxidation signal of $Zn(bpy)_3^{2+}$ and $Cd(bpy)_3^{2+}$ in liquid sulfur dioxide at −70 °C: (background electrolyte, 0.1 M $(TBA)PF_6$: (a) 5 mM $Zn(bpy)_3(PF_6)_2$ (scan rate, 0.15 V s^{-1}; working electrode, 0.5-mm Pt disk), where the lower curve is the theoretical voltammogram (see text); (b) 5.2 mM $Cd(bpy)_3(PF_6)_2$ (scan rate, 10 V s^{-1}; working electrode, 25-μm Pt disk); (c) 2.2 mM $Cd(bpy)_3(PF_6)_2$ (scan rate, 0.5 V s^{-1}; working electrode, 0.5-mm Pt disk); (d) 6.9 mM $Cd(bpy)_3(PF_6)_2$ (scan rate, 0.5 V s^{-1}; working electrode, 0.5-mm Pt disk).

(5) Ferguson, J.; Herren, F. *Chem. Phys.* **1983**, *76*, 45.

peak currents (i_{pa}) were directly proportional to $Zn(bpy)_3(PF_6)_2$ concentration and to $v^{1/2}$. The anodic peak potentials (E_{pa}), as well as the potentials of the inflection points (E_{ifa}), were scan rate independent and the ratio of the cathodic to the anodic peak current (i_{pc}/i_{pa}) was essentially unity. The reversible half-wave potentials for the first and the third redox system were calculated as[6] $E_{pa} - 1.109RT/F$ and $E_{pc} + 1.109RT/F$, respectively. For the second oxidation reaction, which had no well-defined peak potentials, the arithmetic mean of the inflection point potentials $((E_{2ifa} + E_{2ifc})/2)$ was employed in the calculation (see Figure 2a). However, calculation of the theoretical voltammogram, corresponding to a superposition of three reversible systems with reversible half-wave potentials determined as above, produced a voltammogram (Figure 2a) with better resolved peaks than the experimental one. The diffusion coefficient of $Zn(bpy)_3^{2+}$ calculated from experimental voltammograms yielded 2.2×10^{-6} $cm^2\ s^{-1}$, which is in good agreement with the values determined previously[2a,3] for other bpy complexes of divalent transition metal cations in liquid SO_2. Scanning over a potential range of 0–2.7 V for a long time sometimes resulted in the formation of a layer that blocked the electrode surface. This film formation may be partially responsible for the deviation of the experimental signal from theoretical predictions (Figure 2a). The reversible behavior of the first group of peaks persisted up to scan rates as high as 50 V s^{-1}, but at higher scan rates, oxidation peaks were shifted to more positive potentials and the reduction peaks to less positive ones, indicating perhaps some quasireversibility of the electron-transfer reactions under these conditions. Assuming that all three processes have identical standard rate constants (k°) and transfer coefficients (α) equal to 0.5, we estimate a k° value of at least 1.5 cm s^{-1} by the method of Nicholson and Shain.[6] However, this value should be taken as only the lower limit of the rate constant, since the relatively high resistivity of the liquid SO_2 solutions may produce some uncompensated ohmic drop, even when ultramicroelectrodes are used.

The first oxidation waves of $Cd(bpy)_3^{2+}$ (Figure 1b) at low scan rates occurred at potentials slightly less positive than those of $Zn(bpy)_3^{2+}$. The reproducibility of the Cd CV was poorer than those of the Zn complex. The shape of the oxidation peak (Figure 1b) suggested multiple electron-transfer reactions, but the cathodic currents on the reverse scan were significantly lower than predicted for reversible systems (Figure 2c,d). At higher scan rates ($v \geq 5$ V s^{-1}), however, a reversible voltammogram that appeared to be the superposition of three anodic and three cathodic peaks (Figure 2b) could be recorded. In this case, the separation between the consecutive oxidation potentials (79 mV) was smaller than that for $Zn(bpy)_3^{2+}$ oxidation (Table I). The lower limit of k° estimated from the fast scan voltammetry was 0.1 cm s^{-1}, i.e., at least an order of magnitude lower than the value obtained for $Zn(bpy)_3^{2+}$ oxidation. This unexpectedly low rate of $Cd(bpy)_3^{2+}$ oxidation may be attributed to the blocking of the electrode surface by the products of oxidation of free bpy released as a result of partial dissociation of the complex in the solution phase (see below). In fact, the background currents at potentials less positive than those corresponding to the complex oxidation were slightly higher in the presence of $Cd(bpy)_3(PF_6)_2$ than they were with $Zn(bpy)_3(PF_6)_2$, in accordance with the expected difference in stability of both complexes.[7] Poor separation of the peaks corresponding to consecutive oxidation reactions, as well as poor reproducibility of the voltammograms, made the interpretation of the results difficult. Within experimental error, the anodic peak current was linearly dependent on the $Cd(bpy)_3^{2+}$ concentration, while the ratio of the cathodic peak current to the anodic peak current decreased with increasing concentration of $Cd(bpy)_3^{2+}$ (Figure 2c,d). These findings suggest the occurrence of follow-up second- or higher-order processes of a nonregenerative nature. The i_{pa} vs $v^{1/2}$ plots were nonlinear at slow scan rates (Figure 3). The currents measured at 0.03–0.05 V s^{-1} were comparable to those measured for the zinc complex, while those measured at higher scan rates, when the Cd complex oxidation was reversible, were about 40% lower than the corresponding $Zn(bpy)_3^{2+}$ oxidation currents. This difference most probably results from partial dissociation of the complex and partial blocking of the electrode surface by the adsorbed products of bipyridine oxidation occurring at less positive potentials than oxidation of the complex (see below).

The second, totally irreversible anodic signal seen on voltammograms of both Zn and Cd complexes (Figure 1), close to the anodic background limit, was not studied in detail. The positions and the peak heights observed for the Zn complex oxidation were very irreproducible, possibly because of the formation of a blocking film on the electrode surface, which also contributed to the decrease of cathodic currents corresponding to three reversible

Table I. Summary of Physicochemical Data for the Tris(2,2′-bipyridine) Complexes of Zn and Cd in Various Oxidation States

metal complex	$10^6 D$,[a] $cm^2\ s^{-1}$	E°,[b] V	$k_2/10^{-2}\epsilon$,[c] cm s^{-1}	k_2,[d] $M^{-1}\ s^{-1}$	abs[e] max, nm
$Zn(bpy)_3^{2+}$	2.2 ± 0.4	2.33 ± 0.01			
$Zn(bpy)_2(bpy^{\cdot+})^{3+}$		2.43	2.72	70	378 (4780)
			2.46		391 (8790)
			2.25		762 (2570)
			2.04		
$Zn(bpy)(bpy^{\cdot+})_2^{4+}$		2.52			
$Cd(bpy)_3^{2+}$	2	2.31 ± 0.01			
$Cd(bpy)_2(bpy^{\cdot+})^{3+}$		2.39			
$Cd(bpy)(bpy^{\cdot+})_2^{4+}$		2.47			

[a] Diffusion coefficient. [b] Standard potential for the M^+/M couple, where M is the complex in the first column referenced versus the ferrocenium/ferrocene couple. [c] Ratio of the dimerization rate constant and molar absorptivity at 762 nm (see text) listed in order for 0.1 M $(TBA)PF_6$, 0.2 M $(TBA)PF_6$, 0.1 M $(TBA)AsF_6$, and 0.2 M $(TBA)AsF_6$. [d] Apparent dimerization rate constant (see discussion section). [e] Values in parentheses are molar absorptivities expressed in $M^{-1}\ cm^{-1}$.

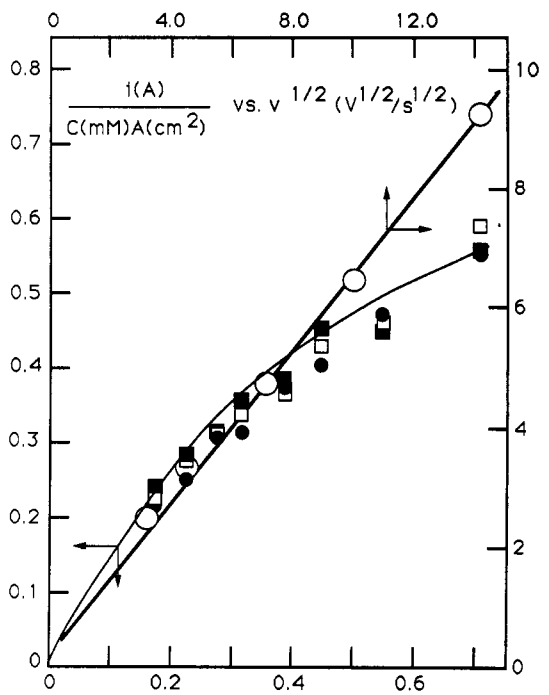

Figure 3. Anodic peak current normalized for the complex concentration and the surface area of the electrode versus the square root of the scan rate for the oxidation of $Cd(bpy)_3(PF_6)_2$ in liquid SO_2 at −70 °C. Background electrolyte: 0.1 M $(TBA)PF_6$. Working electrode: 25-μm Pt disk (open circles) or 0.5-mm Pt disk (remaining symbols). Concentration of $Cd(bpy)_3(PF_6)_2$: 5.2 mM (open circles); 2.2 mM (full circles); 6.9 mM (open squares); 9.6 mM (full squares).

(6) Nicholson, R. S.; Shain, I. *Anal. Chem.* **1964**, *36*, 706.
(7) *Critical Stability Constants*; Smith, R. M., Martell, E. M., Eds.; Plenum Press: New York and London, 1975; Vol. 2, p 236.

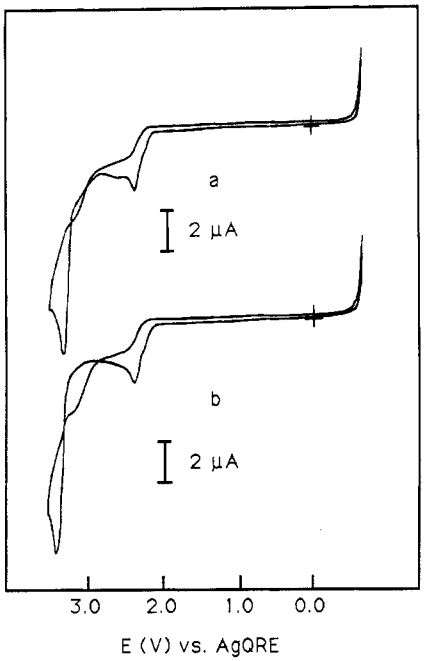

Figure 4. Voltammograms for 6.9 mM $Cd(bpy)_3(PF_6)_2$ solution in liquid SO_2 at −70 °C: (a) first scan; (b) second scan. Background electrolyte: 0.1 M $(TBA)PF_6$. Scan rate: 0.03 V s^{-1}.

electron-transfer processes, when scan reversal occurred in the potential range of the totally irreversible oxidation (Figure 1). The electrode covered with the film could be cleaned by holding the working electrode at potentials more positive than the anodic background limit for several seconds. Sometimes, however, the passivation of the electrode was such that a fresh surface could only be attained by polishing the electrode. Better reproducibility was found for $Cd(bpy)_3^{2+}$ oxidation. Here, surface processes at very positive potentials caused a hysteresis in CVs recorded at low scan rates, especially at higher concentrations of $Cd(bpy)_3^{2+}$ or with multiple scan voltammetry (Figure 4).

The CV of uncoordinated bpy was much less well-defined. The major signals seen on slow scan rate voltammograms (0.03–0.5 V s^{-1}) of 2–7 mM solutions of 2,2′-bipyridine were four irreversible peaks at approximately 1.8, 2.3, 2.8, and 3.4 V vs AgQRE (Figure 5a). The peak current of the first peak (+1.8 V) was linearly dependent on $v^{1/2}$ up to 0.5 V s^{-1}. Application of high scan rate voltammetry ($v \geq 5$ V s^{-1}) employing ultramicroelectrodes revealed that oxidation currents of bpy under these conditions were lower than predicted from extrapolation of the linear i_p vs $v^{1/2}$ plot obtained at the low scan rates. For example, i_{pa} at 200 V s^{-1} at a 25-μm Pt microdisk was about half of that expected from this extrapolation. Although this behavior could suggest an ECE-type mechanism for the reaction, no cathodic peak associated with this oxidation was detected (see below), and the current measured at 200 V s^{-1} was also significantly lower than expected for a simple one-electron irreversible oxidation. The general behavior suggested the formation of a blocking film on the electrode surface on oxidation of bpy. At higher scan rates ($v \geq 50$ V s^{-1}), two additional anodic signals could be seen on the voltammograms. The first one, at around +0.8 V vs AgQRE (Figure 5b), was broad and irreproducible and there was no cathodic peak associated with it even at the highest scan rates applied (10 000 V s^{-1}). The behavior of the second peak, at more positive potentials, suggested its adsorptive nature. A corresponding cathodic peak could also be detected (Figure 5b). This cathodic peak could be observed at scan rates as low as 50 V s^{-1} and was the only cathodic signal detected with fast scan voltammetry with scan rates up to 10 000 V s^{-1} within the potential range −0.5 to +4.5 V vs AgQRE. The pulse radiolysis experiments discussed below indicate that the lifetime of the bpy radical cation in CH_2Cl_2 is 1.2 μs. The effective time scale for CV at 50 V s^{-1} (on the order of RT/Fv) is about 0.5 ms, so the observed cathodic

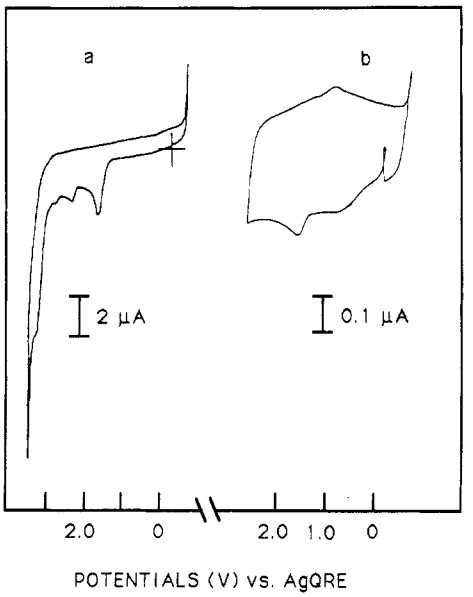

Figure 5. Voltammograms for bipyridine solutions in liquid SO_2 at −70 °C: (a) 4.5 mM bpy, 0.1 M $(TBA)PF_6$ (scan rate, 0.5 V s^{-1}; working electrode, 0.5-mm Pt disk); (b) 7.3 mM bpy, 0.1 M $(TBA)AsF_6$; (scan rate, 5000 V s^{-1}; working electrode, 25-μm Pt disk).

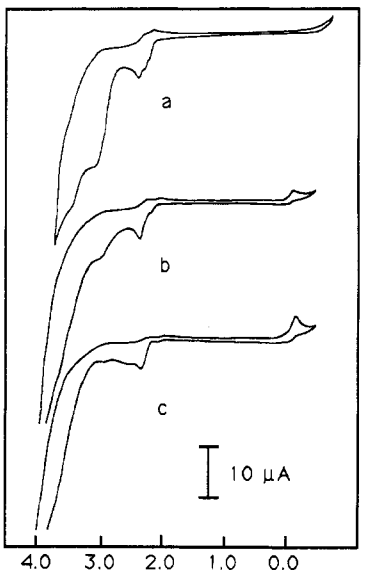

Figure 6. Voltammograms of 8.8 mM solution of $Zn(bpy)_3(PF_6)_2$ in liquid SO_2 at −70 °C after partial oxidation at +2.6 V vs AgQRE. Background electrolyte: 0.1 M $(TBA)PF_6$. Scan rate: 0.2 V s^{-1}. Working electrode: 0.5-mm Pt disk. Fractions of charge corresponding to complete three electron oxidation: 0% (a); 33.3% (b); 101% (c).

wave can hardly be attributed to $bpy^{\bullet+}$ reduction, even when the temperature effect on the $bpy^{\bullet+}$ decay kinetics is taken into account. The observed filming phenomenon and generally poorly defined behavior discouraged us from pursuing the CV of uncoordinated bpy in greater detail.

Bulk Electrolyses. At the beginning of the bulk electrolysis at +2.6 V vs AgQRE, the initially colorless $Zn(bpy)_3^{2+}$ solution showed a blue coloration that underwent subsequent changes to green, greenish brown, and eventually brown. The measured current did not decay to background levels after an amount of charge corresponding to a three-electron oxidation passed. The voltammograms recorded for partially oxidized $Zn(bpy)_3^{2+}$ solutions are shown in Figure 6. In addition to an irreversible oxidation at a potential similar to that of $Zn(bpy)_3^{2+}$, an irreversible reduction at about 0 V vs AgQRE appeared. The latter probably corresponds to H^+ reduction, based on previous results.[4a]

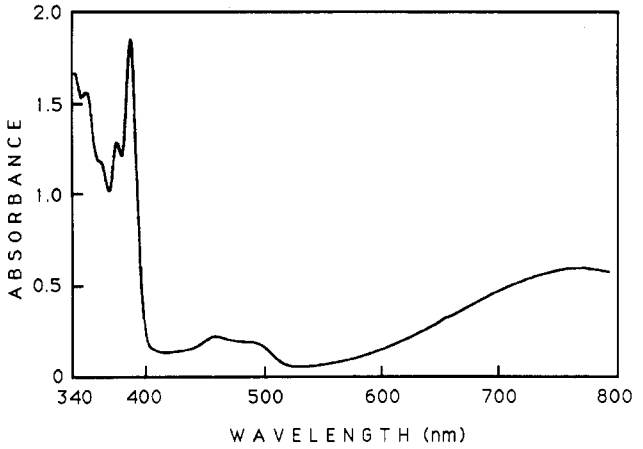

Figure 7. Spectrum of $Zn(bpy)_2(bpy^{\bullet+})^{3+}$ generated electrochemically in 6.5 mM solution of $Zn(bpy)_3(PF_6)_2$ in liquid sulfur dioxide at −70 °C corrected for the absorption of the solvent. Background electrolyte: 0.1 M $(TBA)PF_6$.

The exhaustive electrolysis of yellowish solutions of bpy at a potential more positive than the first oxidation peak resulted in formation of a pale brownish-yellow solution. The electrolysis current decayed to background levels after approximately 50% of the charge corresponding to a one-electron oxidation passed. However, the first oxidation peak could still be observed in the voltammogram of the electrolyzed solution taken with a fresh small electrode, suggesting irreversible passivation of the working electrode during the electrolysis.

Spectroelectrochemistry. In most spectroelectrochemical experiments with $Zn(bpy)_3^{2+}$ solutions, the blue species initially formed on oxidation was generated and its properties studied under various conditions. A typical spectrum of the blue solution is shown in Figure 7. The bands centered at 391 and 378 nm, as well as the broad band at 762 nm, were attributed to the blue species, while the band at about 340 nm corresponded to a more stable product or byproduct of the electrolysis. The small band centered around 450–500 nm may also originate from the presence of the primary product of the electrolysis, but its weak intensity as well as the presence of a similar band in the spectra of more highly oxidized solutions (see below) prevented definite assignment. An essentially identical spectrum was obtained irrespective of whether the generation potential corresponding to three-, two-, or one-electron oxidation of $Zn(bpy)_3^{2+}$ was applied. This spectrum (Figure 7) closely resembles the spectrum of biphenyl cation radical.[8] Such close similarity would be expected if $bpy^{\bullet+}$ in its planar or nearly planar form were the absorbing particle, since the energies and shapes of π orbitals in biphenyl and bpy molecules are very similar.[9] Consequently, it seems reasonable to assign the blue species generated to $Zn(bpy)_2(bpy^{\bullet+})^{3+}$. Higher oxidized 4+ and 5+ forms are kinetically unstable in the presence of an excess of $Zn(bpy)_3^{2+}$ and cannot be observed on the time scale of our spectroelectrochemical experiment (see below). The above assignment is supported by the CV results that show that only three electrons could be removed reversibly from the $Zn(bpy)_3^{2+}$ complex ion. Although the spectra of the more highly oxidized 4+ and 5+ forms might be similar, the electrochemical results suggest that both $Zn(bpy)(bpy^{\bullet+})_2^{4+}$ and $Zn(bpy^{\bullet+})_3^{5+}$ are kinetically unstable in the presence of an excess of $Zn(bpy)_3^{2+}$. From our CV results, the lifetime of $Zn(bpy)(bpy^{\bullet+})_2^{4+}$ and $Zn(bpy^{\bullet+})_3^{5+}$ generated under our experimental conditions are of the order of 1 and 0.1 s, i.e., too short to be observed on the time scale of our spectroelectrochemical experiment (see below).

The decay of $Zn(bpy)_2(bpy^{\bullet+})^{3+}$ was studied by generating a given amount of this species, stopping the electrolysis, and recording a spectrum every 5 s between 340 and 800 nm. However, a kinetic analysis at the single wavelength 762 nm corresponding to the maximum of the visible band was selected. The band in the UV region was less suitable for this purpose because of the gradual irreversible increase in the absorption in the UV region during a long time generation of $Zn(bpy)_2(bpy^{\bullet+})^{3+}$. Either $(TBA)AsF_6$ or $(TBA)PF_6$ were employed as background electrolytes in these experiments. A decay second-order with respect to $Zn(bpy)_2(bpy^{\bullet+})^{3+}$ was observed in most cases. In a few cases, the absorbance decay was faster with apparent first-order kinetics. We believe this first-order decay occurs when contamination of the working electrode compartment with the substances generated at the counterelectrode occurs. From the slopes of the linear plots of the reciprocal absorbance at 762 nm vs time (Figure 8) values of $k_2/\epsilon\ell$ could be obtained, where k_2 is the second-order rate constant, ℓ is the thickness of the solution layer in the cell, and ϵ is the molar absorptivity (assuming only one species contributes to absorption at 762 nm and it is involved in only the second-order decay). The k_2/ϵ values are listed in Table I. The steady-state absorbance, A^∞, found during generation of $Zn(bpy)_2(bpy^{\bullet+})^{3+}$ (under conditions where the rate of generation, i/FV, equals the rate of decay, $k_2(C^\infty)^2$, where i is the current, F is the Faraday constant, V is the cell volume, and C^∞ is the steady-state concentration) is given by

$$A^\infty = \epsilon\ell(i/k_2FV)^{1/2} \quad (1)$$

Separate values of k_2 and ϵ can be obtained from A^∞ and the value of k_2/ϵ. For an experiment with a 0.1 M $(TBA)PF_6$ solution, values of $k_2 = 70\ M^{-1}\ s^{-1}$ and $\epsilon = 2570\ M^{-1}\ cm^{-1}$ (at 762 nm) were obtained. Because of the irreversible increase in the absorbance in the UV region during a lengthy generation of $Zn(bpy)_2(bpy^{\bullet+})^{3+}$, the same procedure could not be applied to determine molar absorptivities at 378 and 391 nm. These values, however, could be estimated by a comparison of the decay data at these wavelengths and at 762 nm. The ratio of absorbance decrease measured at a sufficiently short time at these wavelengths $\Delta A(\lambda)/\Delta A(762\ nm)$ should also approach the ratio of the corresponding molar absorptivities, since other species contributing to the absorption in UV do not decay or decay at a lower rate. Numerical values of molar absorptivities are listed in Table I. The present results show that neither the nature of the supporting electrolyte anion (PF_6^- vs AsF_6^-) nor its concentration influence significantly the kinetics of the reaction. A small decrease of the slope of $1/A$ vs t was found with an increase in the electrolyte concentration, which may be due to formation of ion associations between $Zn(bpy)_2(bpy^{\bullet+})^{3+}$ and the anions of the supporting electrolyte.

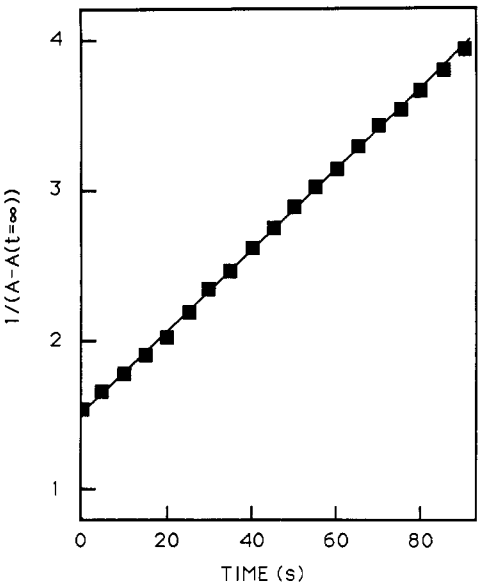

Figure 8. Typical reciprocal absorbance versus time plot for the $Zn(bpy)_2(bpy^{\bullet+})^{3+}$ generated electrochemically in liquid sulfur dioxide at −70 °C. Background electrolyte: 0.1 M $(TBA)PF_6$.

(8) Arai, S.; Ueda, H.; Firestone, R. F.; Dorfman, L. M. *J. Chem. Phys.* **1969**, *50*, 1072.
(9) Gondo, Y. *J. Chem. Phys.* **1964**, *41*, 3928.

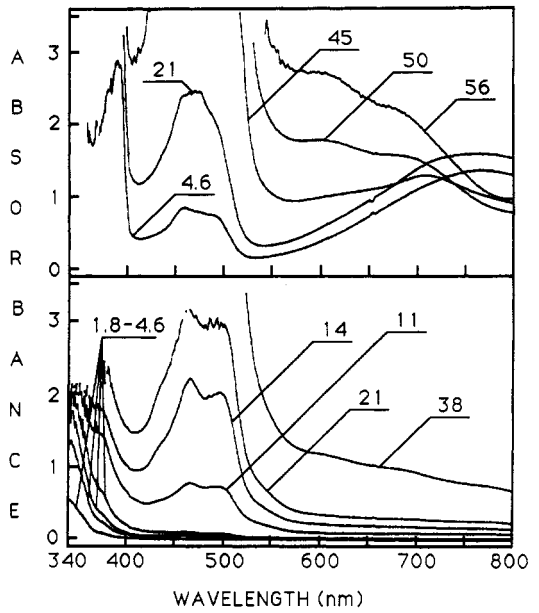

Figure 9. Spectra recorded during the long time electrolysis of 7.9 mM $Zn(bpy)_3(PF_6)_2$ (upper) and 6.4 mM $Cd(bpy)_3(PF_6)_2$ (lower) solutions in liquid sulfur dioxide at −70 °C corrected for the absorption of the solvent. Background electrolyte: 0.1 M $(TBA)PF_6$. Numbers denoting the subsequent spectra are the fractions, expressed as percents, of the theoretical charge corresponding to three-electron oxidations of the complexes.

In accordance with the voltammetric results, we were not able to record the spectrum of the unstable $Cd(bpy)_2(bpy^{\bullet+})^{3+}$ species using our spectroelectrochemical setup. In that case, only experiments were performed in which the spectra of species generated during long time electrolysis were measured. Shown in Figure 9 are the spectra recorded for lengthy oxidations of both $Zn(bpy)_3^{2+}$ and $Cd(bpy)_3^{2+}$ solutions. In both cases, formation of an irregular band centered around 480 nm and weak features at approximately 600 and 670 nm are seen. This result fits our expectations, based on similar properties of both complexes, that similar or even identical oxidation reaction mechanisms should be operative in both cases.

Pulse Radiolysis. We selected methylene chloride as the solvent for pulse radiolysis experiments because an efficient production of cation radicals is expected in this solvent,[8,10] and the solubilities of the metal complexes are higher in CH_2Cl_2 than in other halocarbons. Formation of radical cations in chlorinated hydrocarbons (RCl) upon electron irradiation results from the oxidation of the solute by $RCl^{\bullet+}$ or fragment cations, which, except for secondary electrons, are the primary products of radiolysis.[8] Secondary electrons are easily scavenged by the solvent, probably in a dissociative attachment $RCl + e^- \rightarrow Cl^- + R^\bullet$, and this reaction suppresses the formation of the radical anion.[8] Unfortunately, even in CH_2Cl_2 we were not able to dissolve enough $Zn(bpy)_3(PF_6)_2$ to obtain sufficiently strong signals. The optical densities measured were too close to the noise level, and consequently, not even qualitative data could be obtained for this system. Solubility of $Cd(bpy)_3(PF_6)_2$ in CH_2Cl_2 was much higher, and stronger signals were obtained in this case. However, the results obtained with $Cd(bpy)_3^{2+}$ still suffered from relatively low intensity of signals and poor reproducibility and should be regarded as only semiquantitative. Quantitative results were obtained with bpy solutions, where the signals were sufficiently strong and reproducible. Shown in Figure 10 are transient spectra recorded for a 13.4 mM solution of bpy as well as typical absorbance transients at selected wavelengths. The spectrum of the initially formed short-lived species (Figure 10a) has no visible band similar to that observed for the radical coordinated to the zinc center but is similar to the spectrum of $bpy^{\bullet+}$ in 1,2-dichloroethane reported by Dhanya and Bhattacharyya.[10] The position of the observed UV band correlates with the energy difference between the lowest and one of the higher energy bands in the known photoelectron spectra of bpy.[11] The differences between the spectra of the free and coordinated $bpy^{\bullet+}$ are discussed below.

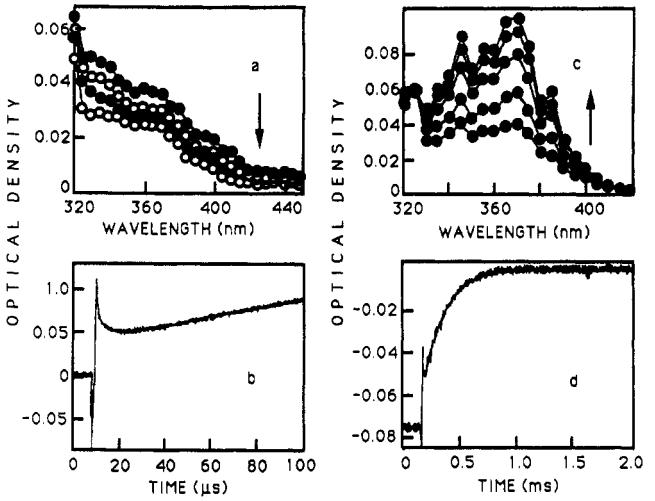

Figure 10. Transient absorption spectra and oscilloscope traces obtained during electron pulse radiolysis of a 13.4 mM solution of 2,2′-bipyridine in anhydrous methylene chloride: (a) spectra recorded 1.1, 2.2, 4.4, and 13.8 μs after application of the electron pulse, where the arrow indicates the direction of change of the optical density with time; (b) oscilloscope trace recorded at 365 nm showing the fast decaying component of the spectrum; (c) Same as part a after 61, 122, 244, 397, and 765 μs; (d) same as part b showing the slow component.

The $bpy^{\bullet+}$ decays (Figure 10b) with the first- or pseudo-first-order rate constant k of $8.4 \times 10^5\ s^{-1}$ (lifetime 1.2 μs) to form a product which undergoes another first- or pseudo-first-order reaction ($k = 5.5 \times 10^3\ s^{-1}$) to give a long-lived product (Figure 10d). The spectrum of this product is shown in Figure 10c.

Only a featureless band centered at approximately 350 nm could be seen in the spectrum of the species generated during the pulse radiolysis of an 8.5 mM $Cd(bpy)_3(PF_6)_2$ solution. The low intensity of the signal did not allow a detailed analysis of the spectrum. The estimated lifetime of the absorbing species was about 25 μs. The similarity of the spectrum to that of free $bpy^{\bullet+}$ rather than $Zn(bpy)_2(bpy^{\bullet+})^{3+}$, as well as the relatively short lifetime of the species generated, suggests that free $bpy^{\bullet+}$ was the primary product generated. Free bpy could be formed by partial dissociation of $Cd(bpy)_3^{2+}$ and, because of its lower oxidation potential, act as a more efficient scavenger than coordinated bpy. The slower decay rate of $bpy^{\bullet+}$ generated under these conditions, compared to $bpy^{\bullet+}$ generated in bpy solutions, could be explained, if radical to parent molecule coupling is mainly responsible for $bpy^{\bullet+}$ decay. The lower concentration of free bpy in $Cd(bpy)_3(PF_6)_2$ solution and slower kinetics of the reaction between $bpy^{\bullet+}$ and coordinated bpy would result in an increase of the $bpy^{\bullet+}$ lifetime.

Discussion

The electrochemical oxidation of the Zn(II) and Cd(II) complexes of bpy in SO_2 can best be described as oxidation of coordinated bpy (as is also proposed for waves of bpy complexes of Fe, Ru, Os, and Ni that occur at similar potentials[2,3]). Coordination of $bpy^{\bullet+}$ to the metal cation changes considerably both its spectral properties and its chemical stability. The UV–

(10) Dhanya, S.; Bhattaharyya, P. K. *J. Photochem. Photobiol. A* **1990**, *54*, 63.

(11) (a) Maier, J. P.; Turner, D. W. *Faraday Discuss. Chem. Soc.* **1972**, *54*, 149. (b) Klasinc, L.; Novak, I.; Rieger, J.; Sholz, M. *Monatsh. Chem.* **1981**, *112*, 697. (c) Barone, V.; Cristinziano, P. L.; Lelj, F.; Pastore, A.; Russo, N. *Gazz. Chim. Ital.* **1982**, *112*, 195. (d) Dobson, B.; Hillier, I. H.; Connor, J. A.; Moncrieff, D.; Scanlan, M. J.; Garner, C. D. *J. Chem. Soc., Faraday Trans. 2* **1983**, *79*, 295.

vis spectrum of electrogenerated $Zn(bpy)_2(bpy^{\bullet+})^{3+}$ species is very similar in the shape and the energy of the bands to the spectrum of the biphenyl radical cation; biphenyl is known to have π electronic properties similar to those of bipyridine.[9] On the other hand, there is no visible band in the spectrum of free $bpy^{\bullet+}$ generated by pulse radiolysis. It is unlikely that this visible band for coordinated $bpy^{\bullet+}$ is due to a charge-transfer transition involving the metal center (i.e., metal to ligand charge transfer, MLCT), given the high third ionization potential of zinc.[12] Moreover, the half-width of this band is too high for intervalence transition to another coordinated bpy.[13] In addition, if the assignments of photoelectron spectra[11] are correct, a similar visible band corresponding to the allowed a_u–b_g (π_3–π_6) transition, centered at about 700–800 nm, would be predicted for the trans π form of the radical, which is not expected to have significantly different π electronic levels than the cis configuration of the radical,[9] where cis and trans pertain to the N-locations assuming some twist around the 2,2′-bond. We suggest then that the spectrum observed for electrogenerated $Zn(bpy)_2(bpy^{\bullet+})^{3+}$ is due to transitions within a planar π form of doubly coordinated $bpy^{\bullet+}$. In fact, the π character of doubly coordinated $bpy^{\bullet+}$ would be expected because of repulsive electrostatic interaction between the metal cation and $bpy^{\bullet+}$, which would make the positive charge of $bpy^{\bullet+}$ more likely to reside on the ring π orbitals than on the nitrogen σ orbitals participating in the metal–ligand bonding. Consequently, the unpaired electron density is expected to be delocalized over the π-electronic system of the bpy ring. The assignments of photoelectron spectra of bpy[11] suggest that the HOMO in bpy is a π orbital, suggesting π character in the free $bpy^{\bullet+}$ as well. In this case, however, a trans configuration of the radical would be expected, similar to that of bpy in an inert solvent[11b,c,14] or in the solid state.[15] Because the energies of π-electronic levels are not expected to differ significantly for both configurations, the lack of a visible band in the spectrum of free $bpy^{\bullet+}$ suggests that the electronic transition corresponding to the visible band in the spectrum of the coordinated $bpy^{\bullet+}$ is either symmetry forbidden in the free $bpy^{\bullet+}$ or shifted significantly to longer wavelengths on decomplexation or there is no such transition in the free $bpy^{\bullet+}$, i.e., the structures of free and coordinated $bpy^{\bullet+}$ differ significantly (e.g., because free $bpy^{\bullet+}$ is a σ-type radical). Because the presence of an allowed π–π transition at a wavelength close to 700–800 nm would be predicted for the trans configuration of $bpy^{\bullet+}$ from the photoelectron spectra,[11] the electronic transition corresponding to the visible band in the spectrum of coordinated $bpy^{\bullet+}$ (cis configuration) probably does not exist in free $bpy^{\bullet+}$ and indicates σ character of the free $bpy^{\bullet+}$ similar to that in the free pyridine radical cation.[16]

The electrochemical and spectroelectrochemical results show that both $Zn(bpy)_2(bpy^{\bullet+})^{3+}$ and $Cd(bpy)_2(bpy^{\bullet+})^{3+}$ are fairly stable in liquid SO_2 and, in opposition to free $bpy^{\bullet+}$ in the presence of excess bpy, their decay is governed by a second-order rate law on the time scale of our experiments. Two possible second-order processes for these highly oxidized radical species are disproportionation and dimerization. However, disproportionation reactions like

$$2Me(bpy)_2(bpy^{\bullet+})^{3+} = Me(bpy)_3^{2+} + Me(bpy)(bpy^{\bullet+})_2^{4+} \quad (2)$$

$$2Me(bpy)_2(bpy^{\bullet+})^{3+} = Me(bpy)_3^{2+} + Me(bpy)_2(bpy^{2+})^{4+} \quad (3)$$

$$2Me(bpy)_2(bpy^{\bullet+})^{3+} = Me(bpy)_3^{2+} + Me(bpy)(bpy^{\bullet+})(R)^{3+} + H^+ \quad (4)$$

where R represents a radical formed by abstraction of H^+ from $bpy^{\bullet+}$, are not consistent with the experimental findings. Reactions 2 and 3 are thermodynamically unfavorable (see the standard potentials in Table I). On the other hand, reaction 4 for $Cd(bpy)_3^{2+}$ should show a hydrogen cation reduction peak[6] in the CV and no such peak was detected. There is H^+ release during exhaustive electrolysis of $Zn(bpy)_3^{2+}$, but the remaining experimental findings suggest that proton release is either a slow process following the second-order reaction or it accompanies further oxidation of primary products of the electrolysis. Consequently, the most probable primary reaction of the coordinated $bpy^{\bullet+}$ is a dimerization reaction. The structure of the reaction product is unknown, but probably carbon–carbon coupling takes place, and eventually, a quaterpyridine molecule, which is partially coordinated to Zn^{2+} and partially protonated, is formed. In the pulse radiolysis experiment, free $bpy^{\bullet+}$ decays according to a different mechanism. The relatively slow dimerization of coordinated $bpy^{\bullet+}$ could be related to strong electrostatic repulsion of highly charged complex ions and steric factors. The differences in the dimerization rates of $bpy^{\bullet+}$ coordinated to different metal centers have not been investigated in depth, but both the present and previous[2,3] results show the same general trend; i.e., a higher stability of $bpy^{\bullet+}$ complexes is observed for metals that form stronger complexes with bpy. The filming found during extended electrochemical oxidation of the complexes and brief oxidation of bpy is consistent with a dimerization step followed by reactions leading to polymer as observed with pyrrole and other heterocyclic compounds.

In a recent paper,[2c] we noted larger differences between the peak potentials corresponding to oxidations of subsequent bpy ligands in Fe(III), Ru(III), and Os(IV) complexes compared to corresponding differences observed for the reductions of coordinated bpy.[1i,j] This phenomenon was qualitatively explained by invoking electrostatic interactions and weaker solvating power of the liquid SO_2 used as a solvent in the oxidation studies[2c] compared to the acetonitrile[1i] or aqueous H_2SO_4[1j] solutions employed in the reduction studies. However, the differences between subsequent oxidation potentials observed for Zn(II) and Cd(II) complexes are smaller than those of the reduction[1i,j] of $Ru(II)(bpy)_3^{2+}$. As opposed to the previous study[2c] where the oxidation state of the metal center was higher than 2+, the present results were obtained for the complexes of the divalent metals. A comparison of the present results with the previous reduction studies[1i,j] suggests, however, that solvation effects are probably not as important as previously thought.[2c] On the other hand the specific effects, e.g., crystal field stabilization energy or π-bonding formation ability may come into play.

Acknowledgment. The pulse radiolysis experiments and analyses of the data produced were performed at the Center for Fast Kinetics Research (CFKR), which is supported jointly by the Biomedical Research Technology Program of the Division of Research Resources of the National Institutes of Health (Grant RR00886) and by The University of Texas at Austin. We appreciate the assistance of Stephan Hubig (CFKR) in the radiolysis experiments. The support of this research by the National Science Foundation (Grant CHE9214480) and the Robert A. Welch Foundation is gratefully acknowledged.

(12) *Standard Potentials in Aqueous Solutions*; Bard, A. J., Parsons, R., Jordan, J., Eds.; Marcel Dekker: New York, 1985; p 24.
(13) Hush, N. S. *Prog. Inorg. Chem.* **1967**, *8*, 391.
(14) (a) Nakamoto, K. *J. Phys. Chem.* **1960**, *64*, 1420. (b) Cumper, C. W. N.; Ginman, R. F. A.; Vogel, A. I. *J. Chem. Soc.* **1962**, *84*, 1188. (c) Castellano, S.; Guenther, H.; Ebersole, S. *J. Phys. Chem.* **1965**, *69*, 4166. (d) Spotswood, T. McL.; Tanzer, C. I. *Aust. J. Chem.* **1967**, *20*, 1227. (e) Galasso, V.; DeAlti, G.; Bigotto, A. *Tetrahedron* **1971**, *27*, 991. (f) Barone, V.; Lelj, F.; Commisso, L.; Russo, N.; Cauletti, C.; Piancastelli, M. N. *Chem. Phys.* **1985**, *96*, 435.
(15) Merrit, L. L., Jr.; Schroeder, E. D. *Acta Crystallogr.* **1956**, *9*, 801.
(16) (a) Shida, T.; Kato, T. *Chem. Phys. Lett.* **1979**, *68*, 106. (b) Rao, D. N. R.; Eastland, G. W.; Symons, M. C. R. *J. Chem. Soc., Faraday Trans. 1* **1984**, *80*, 2803.